PARTICLE IDENTIFICATION BY dE/dx SAMPLING IN NEON

I. Lehraus, R. Matthewson and W. Tejessy
CERN, Geneva, Switzerland

Summary

Systematic studies of identification efficiency for e/π/p were performed in a variety of noble gas mixtures and in pure hydrocarbons at pressures up to 5 atm using a 15 GeV/c tagged beam. Neon mixtures were found to give the best results (6.7 σ π/p separation at 1 atm). Replacing the conventionally used argon by neon would permit a reduction of detector depth by almost a factor of two. The measurements were carried out in a detector with 64 pairs of 2 x 2 cm^2 proportional counters and a 50 cm drift space.

Performance of the neon mixture was verified in a longitudinal drift chamber consisting of 16 stages of 4.7 cm drift each using Flash ADC with 25 ns sampling intervals. The results are similar to those obtained by charge integration over large samples in a detector of the same total length.

Introduction

Efficient particle identification by ionization sampling in the relativistic rise region requires resolution in the 8-9% FWHM range. This is difficult to achieve in a compact colliding beam detector, in which a typical track length will be of the order of 1.5 m. Increasing the operating pressure improves the resolution, but this effect is practically cancelled by a reduction of the relativistic rise slope at high pressures. Therefore, an extensive study of a wide variety of gas mixtures is clearly required to determine the best performance.

Furthermore, optimization of the design parameters of a colliding beam detector demands precision which can only be realized in a full-size detector segment. Indeed, a combination of several secondary effects, which were not even noticed in the first generation of colliding beam devices designed for operation below the minimum of ionization (typical resolution about 15% FWHM), may now appear at a high order level.

The present experiment was dedicated to a detailed study of limits of resolution and linearity of response in various gas mixtures at pressures from 0.5 to 5 atm with up to 50 cm of drift. In addition, a multistage longitudinal drift chamber with fine sampling was used and its performance compared to results obtained by classical charge integration over large samples.

Measurements with 64 samples of 4 cm

The experimental set-up has been described in detail in ref. 1. The detector illustrated in fig. 1 consists of 64 pairs of 2 x 2 cm^2 proportional cells, separated by a double grid from a 50 cm drift space. The cell structure is given in fig. 2. The HV, signal and field wire spacing is 1 cm and the distance between the two separation grids is 0.5 cm. For the signal wires 25 μ diameter stainless steel was chosen. The gas amplification factor was kept in the 10^3 range to assure linear amplitude response. The grid transparency was optimized as shown in the example on fig. 2 by using the beam aligned on the boundary and adjusting the grid potentials. Transparency was always above 0.94. The charges collected by the individual cell pairs were integrated, amplified and processed by a set of 64 ADC's with 8-bit resolution. The measurements were performed at 15 GeV/c in a tagged beam of protons, pions and positrons. The beam spot size was 4 cm FWHM and the momentum bite ± 0.25%. A general description of the measurement procedure and an elaboration of the results for all studied gases is given in ref. 2. Here we put the emphasis on neon mixtures and those aspects of their ionization behaviour that make the use of neon attractive.

The width of the single 4 cm sample dE/dx distribution at 1 atm is plotted in fig. 3, taken from our previous paper[2], for noble gases and pure hydrocarbons. Surprisingly, the results for neon, argon, krypton and xenon show practically the same resolution. Pure hydrocarbons have narrower distributions which, in contrast to the noble gases, improve with increasing molecular weight.

For Ne + 10% C_2H_6, fig. 4 shows an example of truncated mean (lowest 40%) distributions from 64 samples of 4 cm at 1 atm, corrected for individual cell response.

In fig. 5 the final resolution as a function of pressure for 64 x 4 cm samples is shown. At 1 atm the resolutions for Ne, Kr and Xe are all very close to 9.5% FWHM. Using neon instead of argon means a reduction of the detector depth by a factor of 1.7. Neon could thus replace much more expensive krypton and xenon. The hydrocarbons give much better resolution but, unfortunately, their relativistic rise is very low and so the advantage is lost. This is apparent in fig. 6 where the e/p peak ratio at 15 GeV/c is plotted as a function of pressure. As expected, xenon has the highest relativistic rise, followed by krypton. The difference between neon and argon is only about 10%. All hydrocarbons show considerably lower values of relativistic rise.

By expressing the distance between various particle peaks in units of the standard deviation of the final resolution, we obtain the resolving power D/σ. This is plotted in fig. 7 as a function of pressure. At 1 atm neon, krypton and xenon have practically the same merits for π/p separation at about 6.5 σ whereas argon is at the 5.3 σ level. Only ethylene and propane give results comparable to argon. Note that neon at 0.5 atm, which corresponds to about 1.3 m detector depth equivalent, gives (in our particular case) the same result as argon at 2 atm. The e/π separation is at 2.5 σ for neon compared to 3.0 σ for argon. Pure hydrocarbons are grouped at the 1.5 σ level.

Signal attenuation by electron attachment in different gases was measured over 41 cm of drift distance and is shown in fig. 8. Clearly, all noble gases and methane could be used at moderate pressures without problems. Ethylene and ethane are acceptable at atmospheric pressure and propane may still be useful in very small samples.

Drift velocity in neon mixtures

Drift velocity measurements were made in a small test chamber. As shown in fig. 9, saturated drift velocities in the 3-4 cm/μs range can be reached in several neon mixtures already at low E/p values. Low percentages of either propane or isobutane seem to be the most satisfactory. The neon/argon mixtures have the advantage that their density is practically equal to air, which is important in some applications.

Longitudinal drift and fine sampling

This method was originally proposed at BNL[3]. A multistage longitudinal drift chamber was constructed and tested using the same neon mixtures, so that a direct comparison could be made between charge integration over large samples and fine sampling with many small intervals.

The geometry of the detector is presented schematically in fig. 10 where two stages from the total of 16 are shown. In all stages the ionization deposited in the drift space (the 4.7 cm between the 25 μ thick aluminium-foil HV electrode and the grid) was drifted along the particle trajectory into proportional cells of 0.8 x 0.8 cm^2 section. The 15 cm long HV and field wires are 50 μ in diameter, the signal wires are of 10 μ diameter silver plated tungsten. Another foil electrode separates the adjacent stages. Uniform drift field is maintained by a cage structure formed by tubular brass electrodes. The total detector length is 88 cm without the gas tight box. The beam direction was perpendicular to the wires. The triggering scintillation counters were 0.6 cm wide, aligned on the central cells and 3 cm long, covering the middle part of the wires. A veto scintillation counter guarding the full detection area was used to remove background and multiple hits.

A modified circuit of the original fast amplifier developed at BNL (described in ref. 4) was connected as close as possible to the signal wire of each cell. When excited by an input delta function, the shaped output pulse had a rise time of 18 ns, fall time of 26 ns and a FWHM of 32 ns. Single-electron cell response produced a positive 7 mV output signal when the chamber was operated at a gas amplification of 10^4 and the σ_{noise} was 1300 electrons referred to the amplifier input.

The output signals were transmitted via coaxial cables to a 16 channel 6-bit FADC system which was operated continuously with a sample interval of 25 ns. Data were stored in fast 256-bit RAM buffers upon receipt of the event logic decision. Between consecutive particles, these data were transferred to an intermediate buffer until the end of the beam spill, and then read into the on-line computer between ejections.

The 15 GeV/c beam particle flux was kept low to avoid space charge from positive ions and to limit the data transfer load (up to 4000 bytes of information per particle). A dead-time defining veto was provided to prevent pile-up problems.

A typical example of one particle registered in a single stage, using a waveform recorder, is shown in fig. 11. The sampling interval was 10 ns and the drift velocity in Ne + 5% C_2H_6 was 2.2 cm/μs. The spike at the beginning corresponds to the addition of ionization from both sides of the signal wire of the track segment crossing the proportional cell.

Summing up corresponding samples from all 16 stages and for many particles creates the familiar shape shown in fig. 12. The sampling interval was 25 ns and the drift velocity in the Ne + 10% C_3H_8 mixture was about 3.6 cm/μs so that the distance between samples was close to 0.95 mm.

The arrows on fig. 12 indicate the 35 chosen samples on the plateau used for the further data analysis. Single sample distributions for 15 GeV/c protons and positrons are plotted in fig. 13 within the 6-bit FADCs' dynamic range.

The final distributions of mean of 40% smallest values from 560 samples (16 stages of 35) for tagged protons, pions and positrons are plotted in fig. 14. The differences between individual stage responses and the 2-3% droop from sample 16 to 50 were not here corrected. The first effect has only a limited influence on the final distribution - the ionization fluctuations being predominant. The droop is difficult to correct for every individual track due to a dependence on the ionization values registered in the preceding samples.

The results obtained in Ne + 10% C_3H_8 at 1 atm for 560 samples of 0.95 mm interval are summarized as follows:

Resolving power D/σ	Mean of smallest 10%	20%	40%	70%	100%
e/p	3.82	4.60	4.61	4.52	3.42
e/π	1.01	1.18	1.29	1.18	1.18
π/p	2.81	3.42	3.33	3.34	2.24

Conclusions

A new gas mixture containing neon and a low percentage of hydrocarbons (C_2H_6, C_3H_8 or iC_4H_{10}) is proposed for dE/dx sampling applications in the relativistic rise region. Particle identification efficiency in neon was found to be equal to results obtained in xenon and krypton. Note that atmospheric krypton is contaminated by the β-emitting ^{85}Kr isotope which prevents its use in big volume detectors. Use of neon instead of argon opens the possibility to reach 6σ separation for π/p up to about 20 GeV/c in a detector depth below 1.5 m and at atmospheric pressure. At the same time, the radiation length in neon is about 3 times longer than in argon.

Comparing results obtained in identical conditions using charge integration in 64 x 4 cm samples and longitudinal drift with fast sampling in 560 x 0.95 mm intervals, we found similar e/π/p ionization ratios in both cases. On the other hand, the resolving power D/σ was reduced by a factor of two in the longitudinal drift approach. This is in fair agreement with a square root of the total length ratio for the two detectors. It should be remembered that, from the total length of 88 cm for the longitudinal drift chamber, only 60% (i.e. 16 stages x 35 x 0.95 mm) were exploitable for ionization sampling. Some improvement

of the performance of this method is certainly possible, but there seems to be very little difference in the depth required for either of these detectors. For the longitudinal drift resolution no gain is to be expected by increasing the pressure, since for a given maximum sampling rate the amount of ionization deposit between samples is increased in proportion. In the case of inclined and curved tracks the implications of varying interval length during the fine sampling are hard to assess, especially when the average distance between the ionization clusters is of the same order as the diffusion in the gas and the sample interval itself. Furthermore, for the data acquisition and later data analysis it should not be overlooked, that in the longitudinal drift method the amount of data to be processed will vastly increase in comparison to charge integration over large samples.

Acknowledgments

The pressure vessel for the first detector was designed and constructed by G. Linser and G. Schmidlin. We acknowledge the contribution of J.D. Capt in the design and assembly of both detectors and are obliged to Dr. P. Rehak (BNL) for participation in the design of the fast amplifiers for the longitudinal drift detector. We are indebted to E. Chiaveri for tuning and operation of the S3 beam and to the members of the Beam and Detectors Group of the EF Division for their participation in the construction work and during the tests. Continuous support and encouragements from Drs P. Lazeyras and A. Minten were greatly appreciated.

References

1. I. Lehraus et al., CERN/EF 81-4 (1981) (to be published in Nucl. Instr. & Meth. in Phys. Res.).

2. I. Lehraus et al., CERN/EF 82-1 (1982) (to be published in Nucl. Instr. & Meth. in Phys. Res.).

3. T. Ludlam et al., IEEE Trans. Nucl. Sci. NS-28 (1981), No. 1, 439.

4. R.A. Boie et al., IEEE Trans. Nucl. Sci. NS-28 (1981), No. 1, 603.

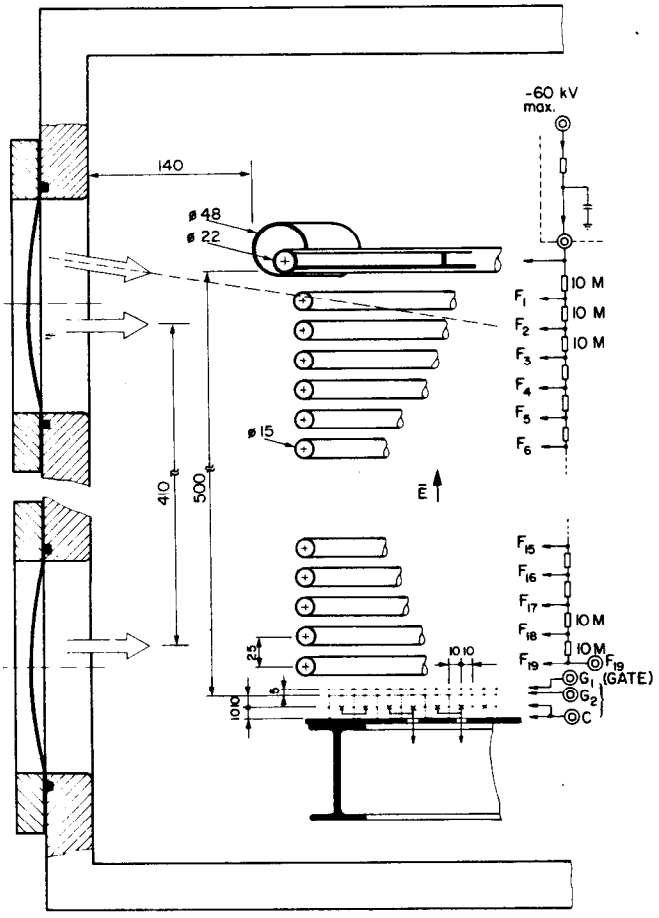

Fig. 1 - Electrode structure of detector used in studies of resolution in various gases and at various pressures. 64 x 4 cm samples, 50 cm drift space.

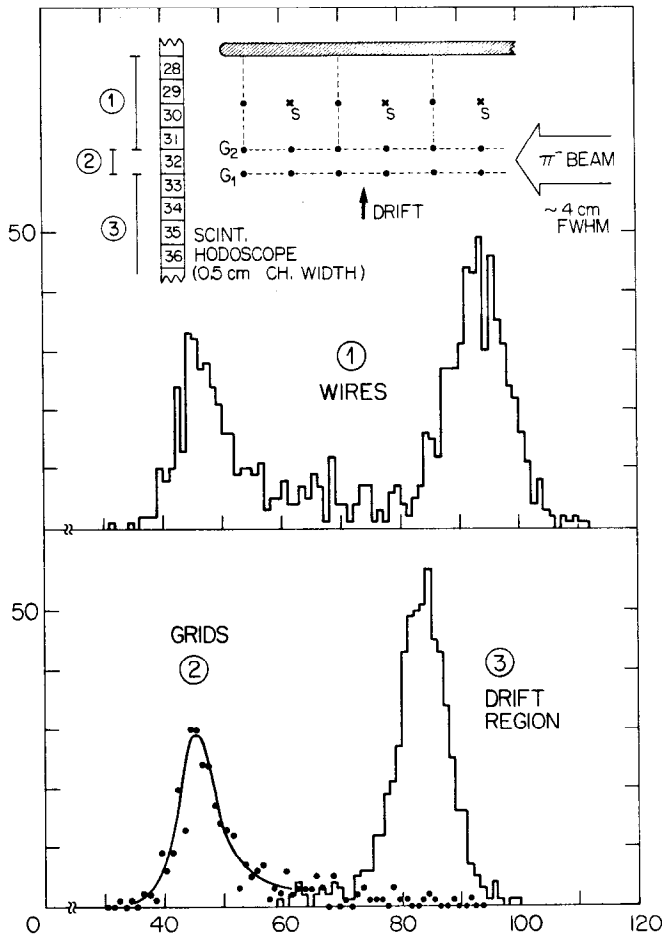

Fig. 2 - Details of the 2 x 2 cm² proportional cell geometry including the separation grids. Example of optimization of grid transparency by adjusting the grid potentials so as to merge the peaks of the truncated mean distributions measured inside the cells (1) and in the drift space (3). Beam aligned on the boundary; the secondary peak (2) comes from the region between the grids.

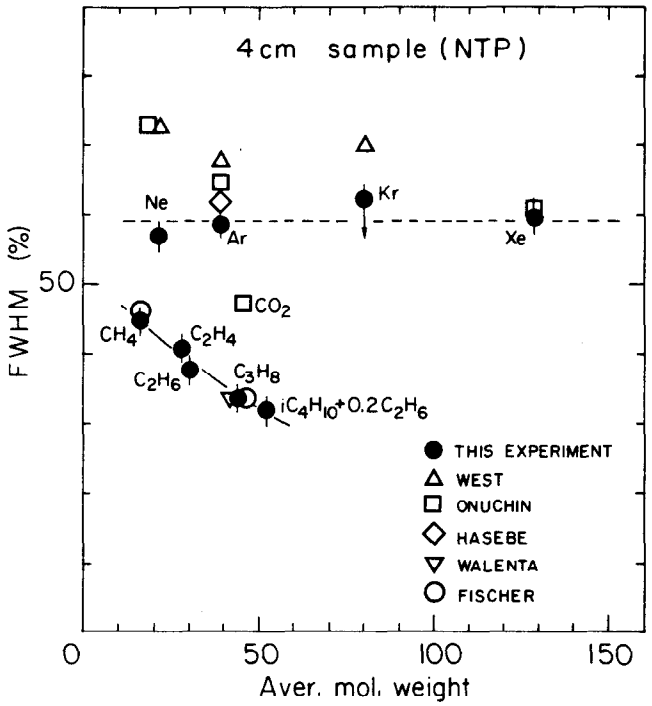

Fig. 3 - Width of the single 4 cm sample distribution for 15 GeV/c pions at 1 atm as a function of average molecular weight of the gas.

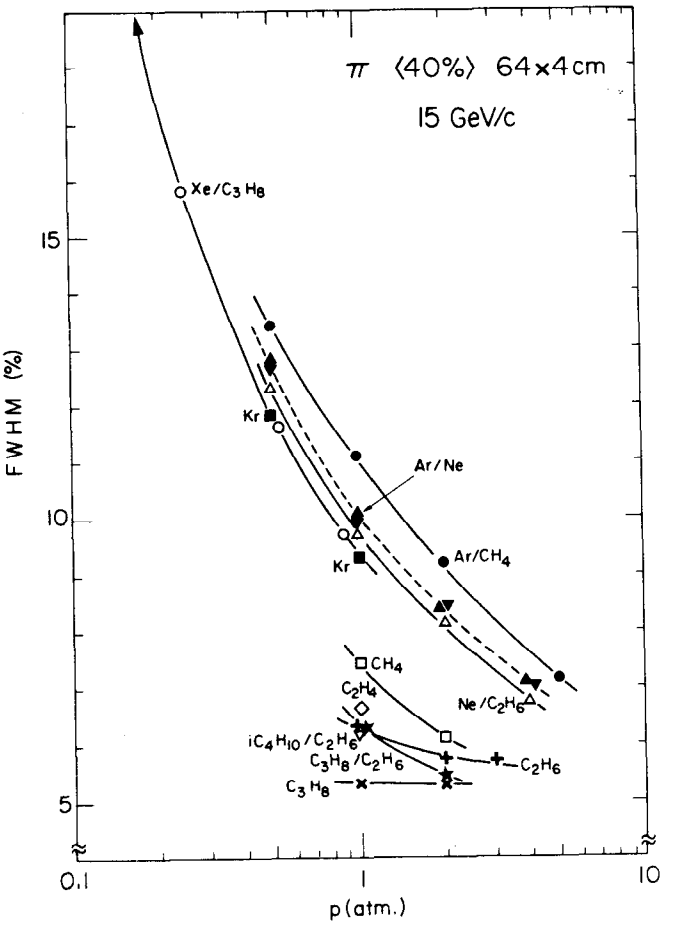

Fig. 5 - Final resolution of mean of smallest 40% of 64 samples of 4 cm for pions at 15 GeV/c as a function of pressure.

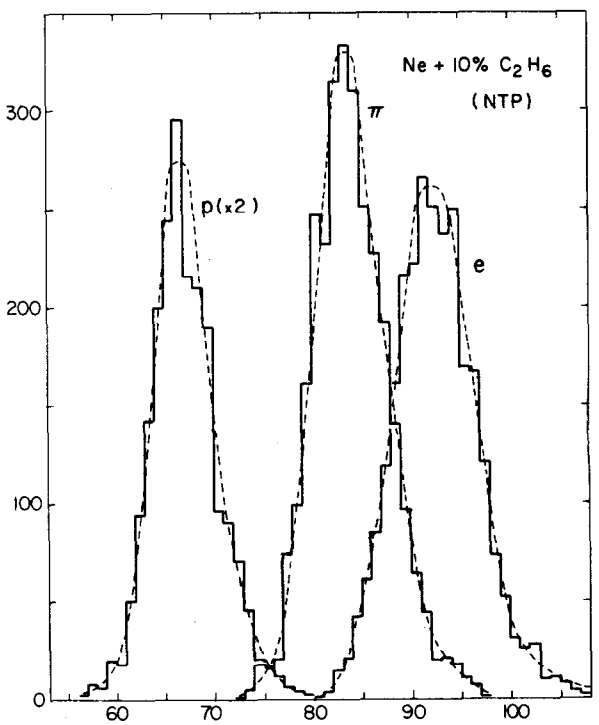

Fig. 4 - Distribution of mean of 40% smallest values of 64 x 4 cm samples in Ne + 10% C_2H_6 at 1 atm. 15 GeV/c tagged protons, pions and positrons.

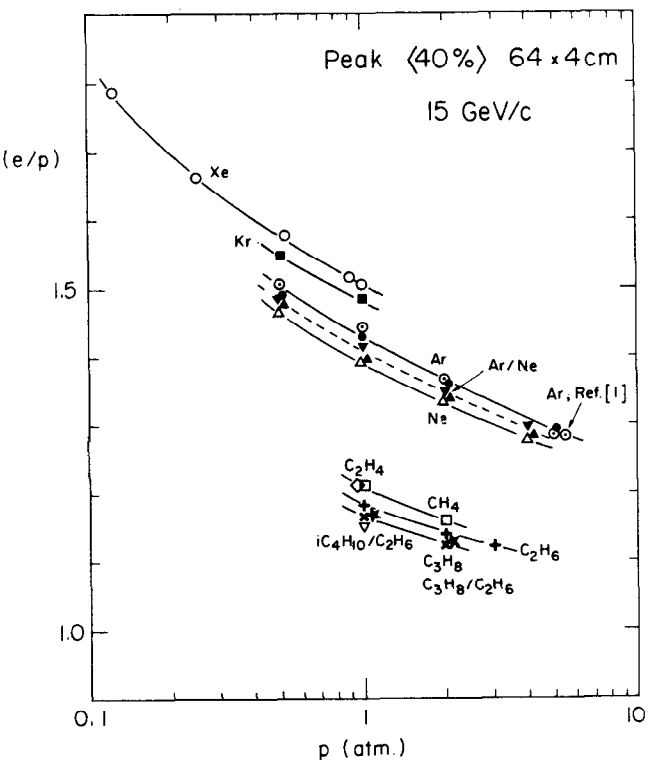

Fig. 6 - Relativistic rise at 15 GeV/c for e/p truncated mean distributions of 64 x 4 cm samples as a function of pressure.

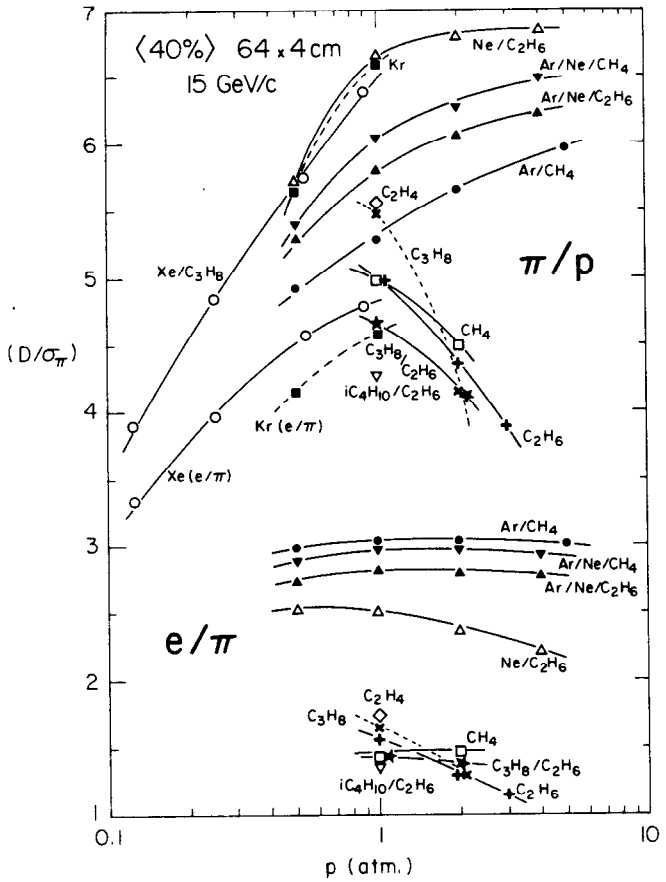

Fig. 7 - Resolving power D/σ for π/p and e/π for various gases as a function of pressure.

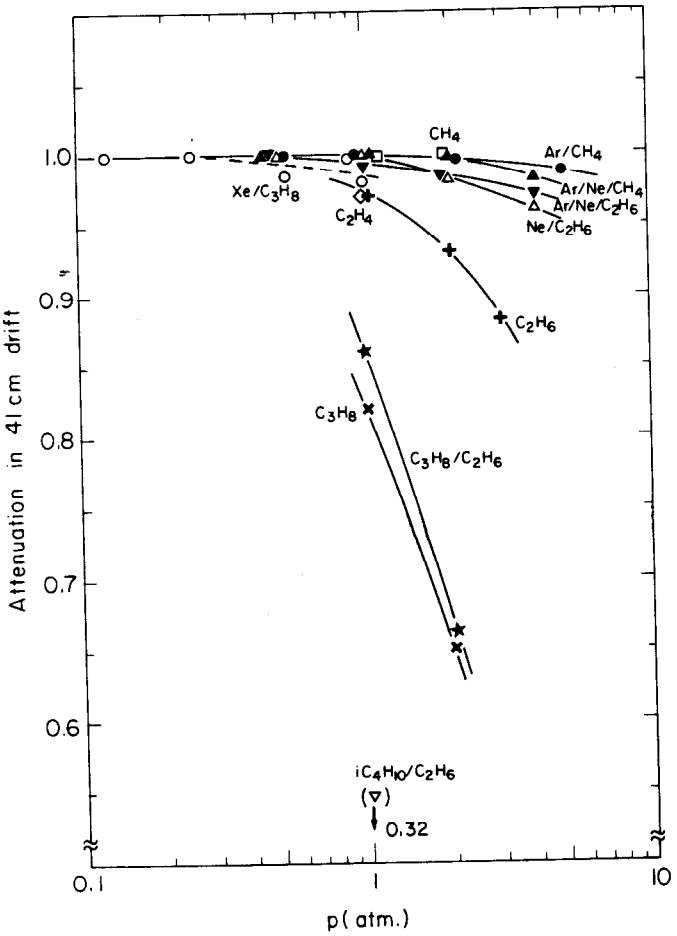

Fig. 8 - Pressure dependence of attenuation over 41 cm in the drift region.

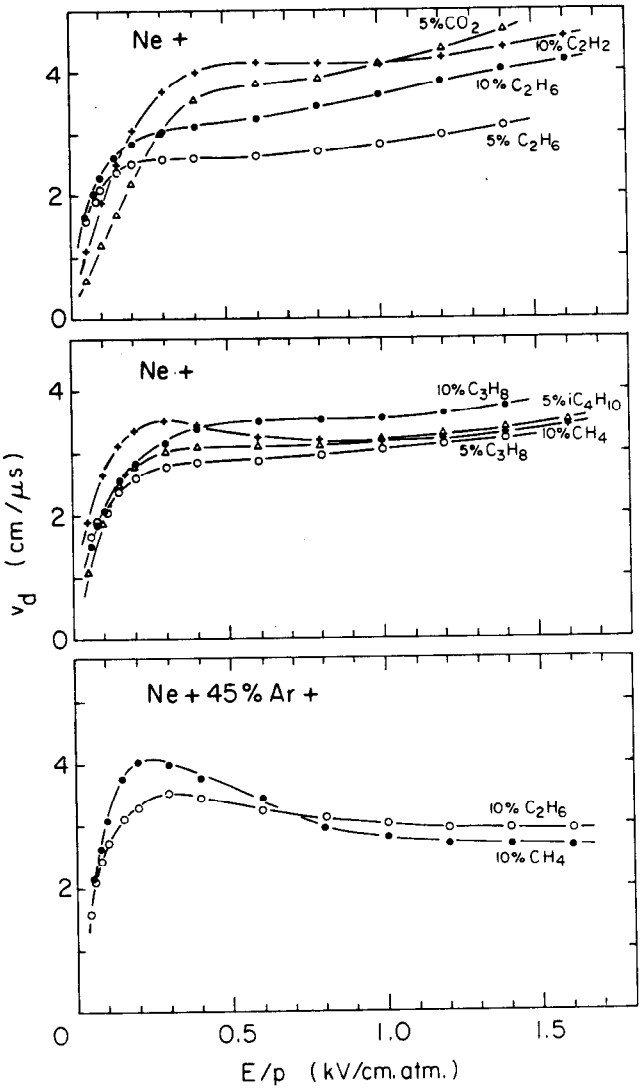

Fig. 9 - Drift velocity for neon and neon/argon with various quenchers.

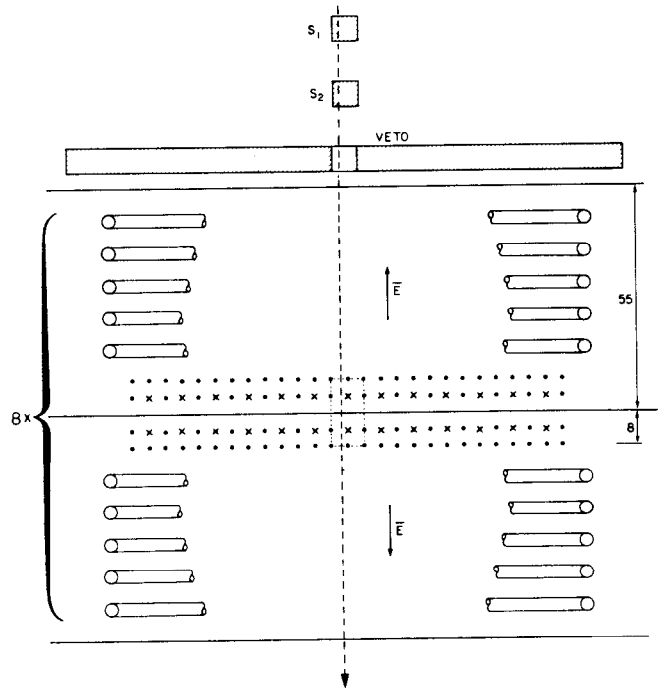

Fig. 10 - Simplified diagram of 2 stages out of the 16 stage longitudinal drift chamber. The alignment of the triggering scintillators on the central cells is schematically shown; the true position of the chamber is between S_1 and S_2.

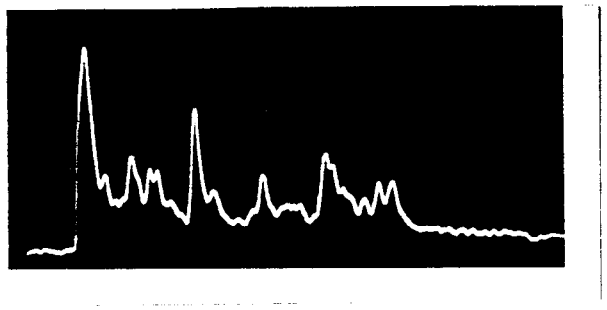

Fig. 11 - Example of a single event in one stage (4.7 cm of drift). Ne + 5% C_2H_6, v_d = 2.2 cm/μs. 10 ns sampling interval.

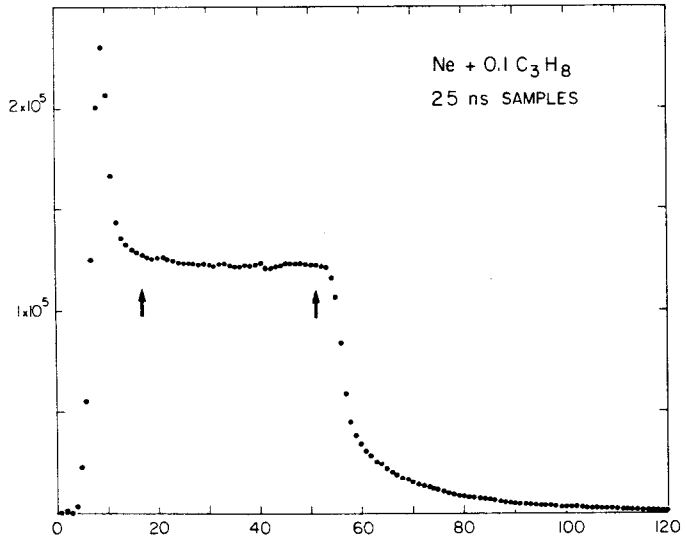

Fig. 12 - Accumulated ionization values for many particles (combined corresponding samples from all 16 stages). Ne + 10% C_3H_8, sampling interval 25 ns. Arrows indicate range of samples used for the data analysis.

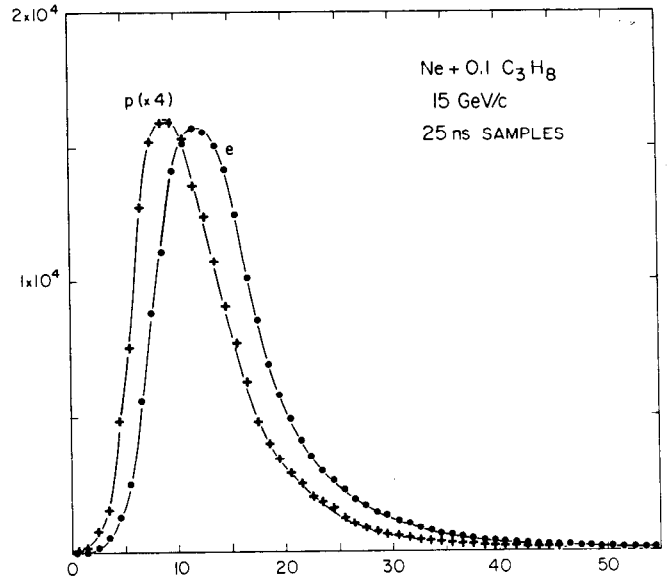

Fig. 13 - Single 25 ns sample distributions using the 35 samples marked in fig. 12 in each of the 16 stages for 15 GeV/c protons and positrons in Ne + 10% C_3H_8.

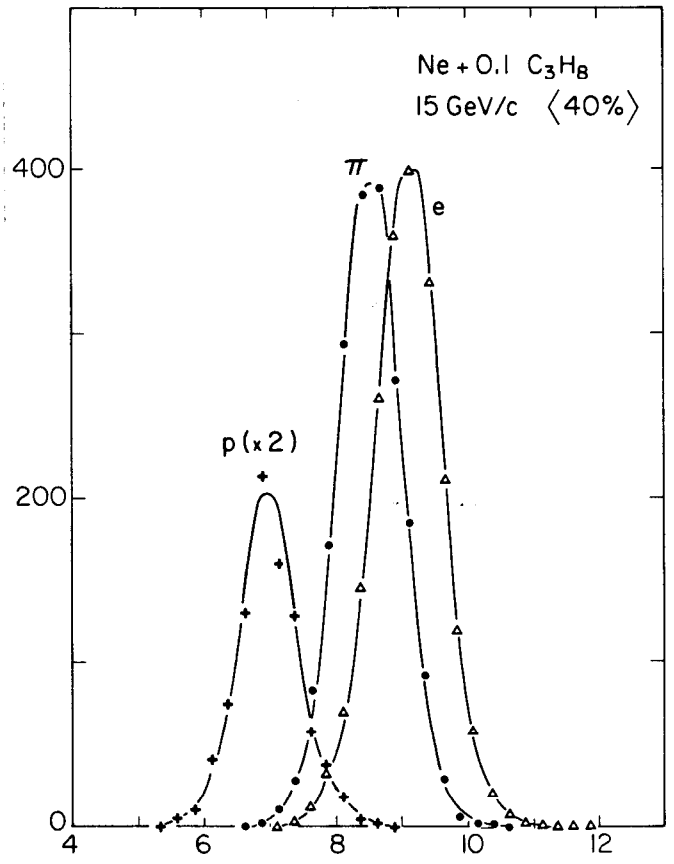

Fig. 14 - Final distribution of mean of 40% smallest values for 15 GeV/c tagged protons, pions and positrons. 560 samples of 25 ns, Ne + 10% C_3H_8.